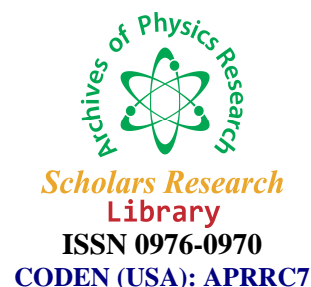




## Scholars Research Library

Archives of Physics Research, 2010, 1 (3):44-53  
(<http://scholarsresearchlibrary.com/archive.html>)



### Optical, thermal, mechanical and electrical properties of a new NLO material: Mono- L-alaninium nitrate (MAN)

M. Vimalan<sup>1\*</sup>, X. Helan Flora<sup>2</sup>, S. Tamilselvan<sup>3</sup>, R. Jeyasekaran<sup>4</sup>, P. Sagayaraj<sup>4</sup>  
and C. K. Mahadevan<sup>1</sup>

<sup>1</sup>Physics Research Centre, S.T. Hindu College, Nagercoil

<sup>2</sup>Department of Physics, Kamaraj College, Tuticorin

<sup>3</sup>Department of Physics, Arignar Anna Government Arts College, Cheyyar

<sup>4</sup>Department of Physics, Loyola College, Chennai

---

#### ABSTRACT

*Semi-organic nonlinear optical single crystals of mono- L-alaninium nitrate (MAN) were grown by the slow evaporation technique. The structure and morphology of the grown crystals were estimated by single crystal XRD analysis. The UV-Vis-NIR spectrum of MAN indicates a wide optical transmission window from 290-2000 nm. The SHG in the sample is confirmed by Nd:YAG laser employing the Kurtz and Perry powder technique and its damage threshold is found to be 7.12 GW/cm<sup>2</sup>. TG and DTA techniques confirm that the sample is structurally stable upto 146 °C. The mechanical properties of the grown crystals are studied using Vickers microhardness tester. Dielectric measurements were carried out and the nature of variation of dielectric constant  $\epsilon_r$  and dielectric loss in the frequency range of 50 Hz to 5 MHz was studied and reported. Photoconductivity studies of mono-L-alaninium nitrate crystal reveal the negative photoconducting nature.*

**Keywords:** Crystal growth from solution; Thermal properties; NLO; Dielectric properties.

---

#### INTRODUCTION

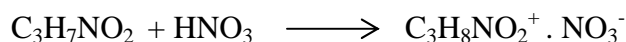
The search and design of highly efficient NLO crystals for visible and ultraviolet (UV) region are extremely important for laser processing. In view of this, there is a demand for new NLO crystals which have a shorter cut-off wavelength. An ideal NLO crystal must possess sufficiently large NLO coefficient, transparency in UV and visible region, high laser damage threshold, greater environmental stability and easy growth with large dimension [1]. In general, most of the organic molecules designed for nonlinear optical (NLO) applications are the derivatives of an aromatic system substituted with donor and acceptor substituents. In the search for new NLO materials with better mechanical properties, many researchers have focused on the small organic molecules having a large dipole moment and a chiral structure, but these attempts in general resulted in environmentally less stable materials. Hence, material scientists are showing

increased attention on semiorganic materials. They have the combined advantages of high optical nonlinearity and chemical flexibility of organic materials with the thermal stability and mechanical robustness of inorganic NLO materials [2-5]. Recent works in this direction have led to the development of several semiorganic NLO crystals belonging to amino acids, particularly the complexes of L-arginine, L-alanine and L-histidine [6-8]. Among the complexes of L-alanine, L-Alaninium oxalate (LAO) and L-alaninium maleate (LAM) are reported to be promising NLO active materials [9-10]. This article deals with NLO single-crystal of mono-L-alaninium nitrate (MAN), which is a recently developed material with the potential for NLO applications. Ivan Nemeč *et al* (1999) found a new class of alanine compounds with nitric acid composition by successfully crystallizing mono-L-alaninium nitrate (MAN) of tiny size ( $0.5 \times 0.4 \times 0.35 \text{ mm}^3$ ). Its empirical formula is  $\text{C}_3\text{H}_8\text{N}_2\text{O}_5$  and the reported cell parameters are  $a = 5.6627 \text{ \AA}$ ,  $b = 7.4705 \text{ \AA}$ ,  $c = 16.1420 \text{ \AA}$  with  $\text{P}2_12_12_1$  space group [11]. The earlier work was confined to the crystal structure and vibration spectra of MAN crystal. The growth of bulk size crystals and their physical properties have not yet been studied. In the present investigation, we are reporting for the first time the growth of MAN crystal in bulk size and its optical, thermal, photoconductivity and dielectric properties. The second harmonic generation in the sample has been confirmed for the first time and its SHG efficiency has been determined. In addition, the damage threshold of MAN has been found out and compared with other NLO crystals.

## MATERIALS AND METHODS

### 2.1 Synthesis and growth of MAN crystal

Mono-L-alaninium nitrate (MAN) was synthesized by dissolving equiv-molar ratio of L-alanine (Merck 99%) and nitric acid (Merck 69%) in double-distilled water at  $30^\circ\text{C}$ . During the reaction period, we have observed that vigorous stirring leads to very low yield of the product, hence the stirring was done slowly for a period of 1 to 2 hours. In addition, the pH of the solution seems to have a definite influence on the reaction process and we found a pH of 4.5 is highly desirable. The following chemical reaction is expected to take place.



The synthesized salt of MAN was obtained by slow evaporation of the solvent.

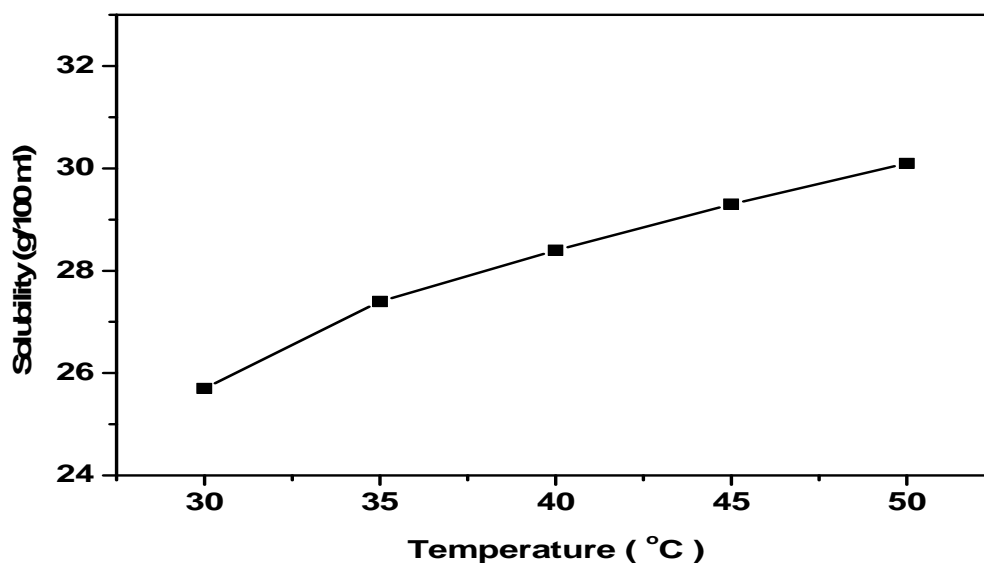


Fig. 1. Solubility curve of MAN

The solubility of product in double distilled water was measured at five different temperatures (30, 35, 40, 45 and 50 °C). The solubility data was determined by dissolving the synthesized salt in 100 ml of double distilled water at a constant temperature followed by mild stirring for 1 hour. After attaining the saturation, the equilibrium concentration of the solute was analyzed gravimetrically. The solubility of MAN (Fig. 1) increases with the temperature and thus exhibits positive solubility coefficient.

In order to achieve the growth of bulk size crystals, saturated solution of mono-L-alaninium nitrate (MAN) was prepared in accordance with the solubility data using the recrystallized salt. Within week time, colourless tiny crystals were formed by spontaneous nucleation. Selected seed crystals with suitable growth habits and good optical transparency were hung into the super saturated solution of mono-L-alaninium nitrate and then covered with perforated lid. After a growth period of 35 days, good quality crystals of dimension upto  $16 \times 6 \times 2 \text{ mm}^3$  were harvested. The photograph (Fig. 2) of as grown mono-L-alaninium nitrate (MAN) crystal suggests the prismatic growth habit of the crystal and it is clearly confirmed in the morphology study. The crystal has six well developed faces, namely,  $(2\ 1\ 1)$ ,  $(0\ 1\ 2)$ ,  $(0\ 0\ 1)$ ,  $(0\ 1\ 0)$ ,  $(0\ 1\ 1)$  and  $(2\ \bar{1}\ 1)$  and they are shown diagrammatically in Fig. 3.

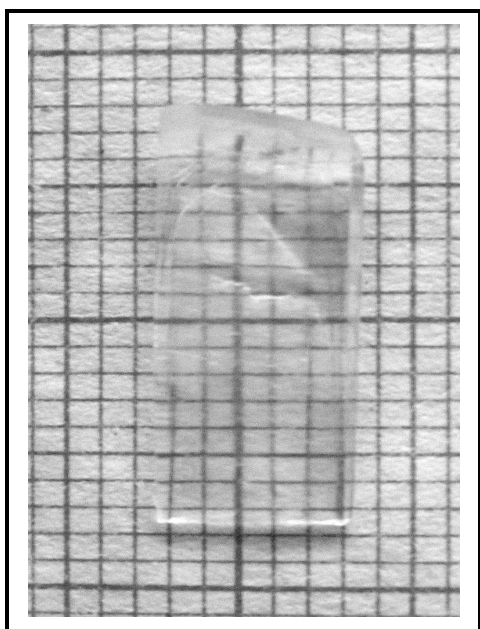


Fig. 2. Photograph of as grown MAN crystal

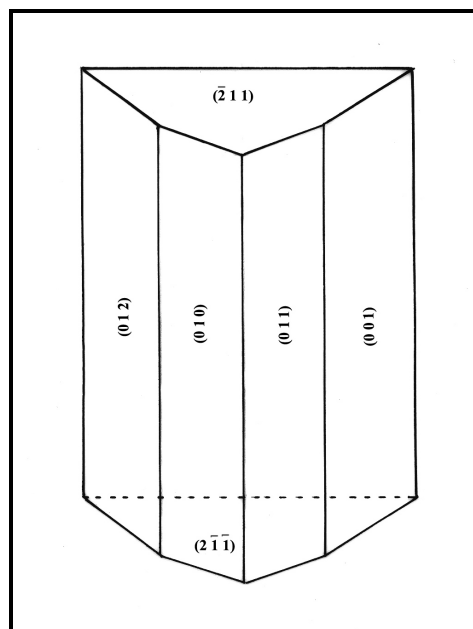


Fig. 3. Morphology of MAN

### Characterization

Single crystal XRD data and morphology of the grown crystal is found out by using ENRAF NONIUS CAD4 single crystal X-ray diffractometer with  $\text{MoK}_\alpha$  ( $\lambda = 0.71073\text{\AA}$ ). The various functional groups present in the sample were identified and confirmed by recording the FT-IR spectrum using BRUKER IFS-66V spectrometer. The optical absorption spectrum of MAN crystal of thickness 2 mm was recorded in the region between 200 and 2000 nm using the VARIAN CARY 5E model spectrophotometer. The SHG efficiency of the sample was measured using Nd:YAG Q-switched mode locked laser ( $\lambda = 1064 \text{ nm}$ ). The thermal behaviour was investigated by NETZSCH STA 409C thermal analyzer. Microhardness study was made using a Vickers microhardness tester fitted with a diamond pyramidal indenter. The dielectric constant and dielectric loss of the sample were measured at different temperatures

using HIOKI 3532-50 LCR HITESTER in the frequency range from 50 Hz – 5 MHz. The photo current and dark current of the sample were recorded using a picoammeter (Keithley 485).

### 3.1 Single crystal XRD analysis

The structure of mono-L-alaninium nitrate (MAN) was solved by the direct method and refined by the full matrix least-squares fit technique employing the SHELXL program. The crystal belongs to orthorhombic structure with  $P2_12_12_1$  space group. The lattice parameters are  $\mathbf{a} = 5.6627 \text{ \AA}$ ,  $\mathbf{b} = 7.4700 \text{ \AA}$  and  $\mathbf{c} = 16.1423 \text{ \AA}$  and the data obtained in the present study is matching well with the literature data [11].

### 3.2 FT-IR analysis

The infrared spectrum of MAN crystal is shown in Fig. 4. The broad and medium-intensity bands in the region  $3200\text{-}2500 \text{ cm}^{-1}$  are characteristic for the stretching vibrations of the N-H and O-H groups connected by hydrogen bonds in the crystal. On the basis of correlation curves between the wavenumber of the O-H vibration and the length of the hydrogen bond, the band corresponding to the O-H...O bonds can be expected at  $2900 \text{ cm}^{-1}$ . Another sensitive band of out-of-plane O-H...O bending vibration is located at  $875 \text{ cm}^{-1}$  (mixed with C-O-H). In the spectrum of LAM, these bands are almost overlapped by the bands of the stretching N-H and O-H vibrations. In the area of antisymmetric and symmetric deformation vibration of the  $\text{NH}_3^+$  group in the FT-IR spectrum, it is possible to observe marked splitting in the wavenumber interval of  $1638\text{-}1513 \text{ cm}^{-1}$ . The presence of alaninium ions in the crystal structure is reflected in the bands of the C-O stretching vibration ( $1416 \text{ cm}^{-1}$ ) and C-O-H in-plane ( $1227 \text{ cm}^{-1}$ ) and out-of-plane ( $875 \text{ cm}^{-1}$ ) bending vibrations. It is assumed that the C-O and C-O-H vibrations are highly mixed.

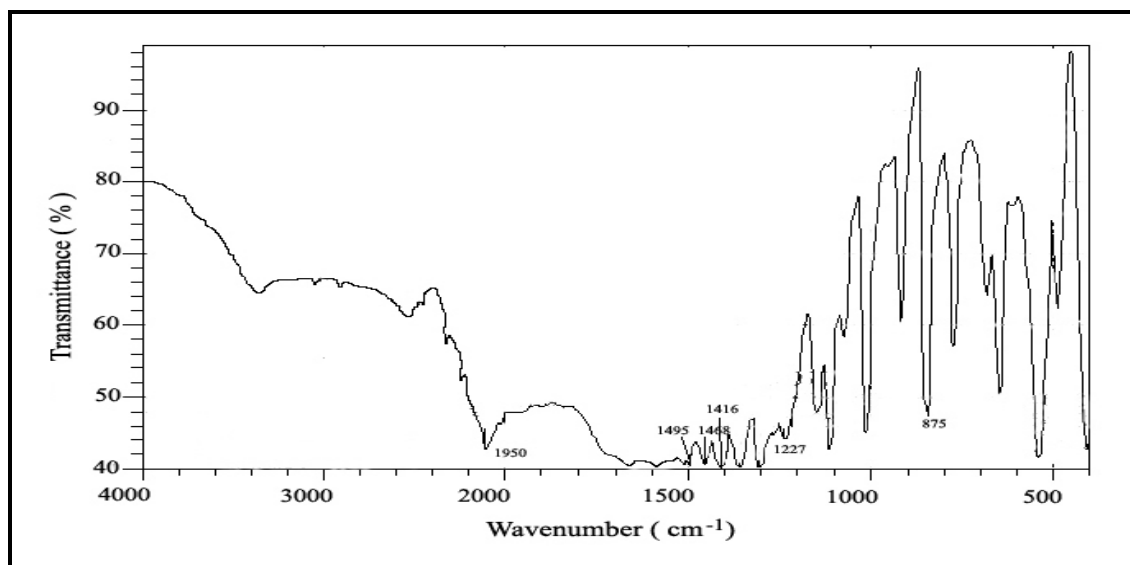


Fig. 4. FT-IR spectrum of MAN

### 3.3 UV-Vis-NIR spectral analysis

The UV-Vis-NIR absorbance spectrum of MAN crystal is shown in Fig. 5, it possesses a low optical absorption starting from UV to the entire visible region. It has less than 0.2 arbitrary unit of absorbance and the lower cut-off wavelength starts at 290 nm. Interestingly, the material has fairly high transparent nature in both UV and visible region and thus making it a potentially useful crystal for NLO application.

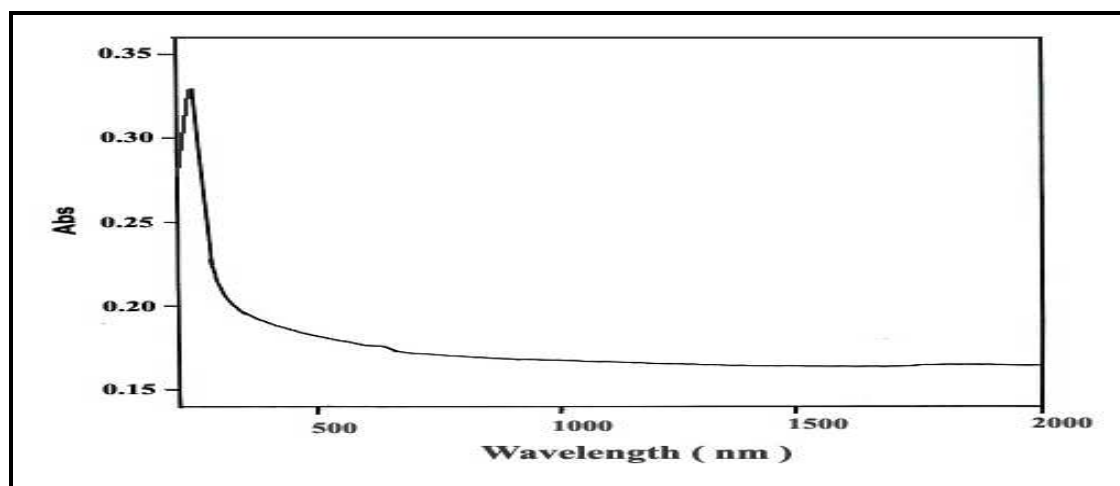


Fig. 5. Optical absorption spectrum of MAN

### 3.4 NLO properties

Kurtz and Perry powder SHG test was carried out on MAN crystal to study its second harmonic generation efficiency. The freshly powdered sample of particle size (above 150  $\mu\text{m}$ ) was illuminated using Q-switched, mode locked Nd:YAG laser with input pulse of 6.2 mJ. The emission of green radiation from the crystal confirmed the second harmonic signal generation in it. A second harmonic signal of 320 mV was obtained for MAN with reference to KDP (124 mV). Thus, the SHG efficiency of the material is nearly 3 times greater than that of KDP and it is also much greater than some of the NLO crystals like LAFB, LHB, LHDN, LAHF and LAA of amino acid family [12-15].

The laser damage threshold study in MAN was made using the above setup in single-shot mode. The laser damage density of the sample was found to be 7.12  $\text{GW}/\text{cm}^2$ . The observed damage threshold value is greater than that of few well-known NLO crystals like KDP, urea and BBO [16].

### 3.5 Thermal analysis

The thermogravimetric and differential thermal analyses of mono-L-alaninium nitrate (MAN) were carried out between 50 and 400  $^{\circ}\text{C}$  in nitrogen atmosphere at a scanning rate of 15  $^{\circ}\text{C}/\text{min}$ . The TG and DTA traces are shown in Fig. 6. A single major weight loss starting at about 210  $^{\circ}\text{C}$  is observed from the TGA trace. The decomposition completes at about 302  $^{\circ}\text{C}$ , leaving no residue. But below 210  $^{\circ}\text{C}$ , there is no weight loss, hence the crystal is completely free of any entrapped or physically adsorbed water. However, the DTA thermogram clearly indicates an endothermic peak appearing at 146  $^{\circ}\text{C}$ , which corresponds to the melting point of the sample and the same has been verified using the melting point apparatus.

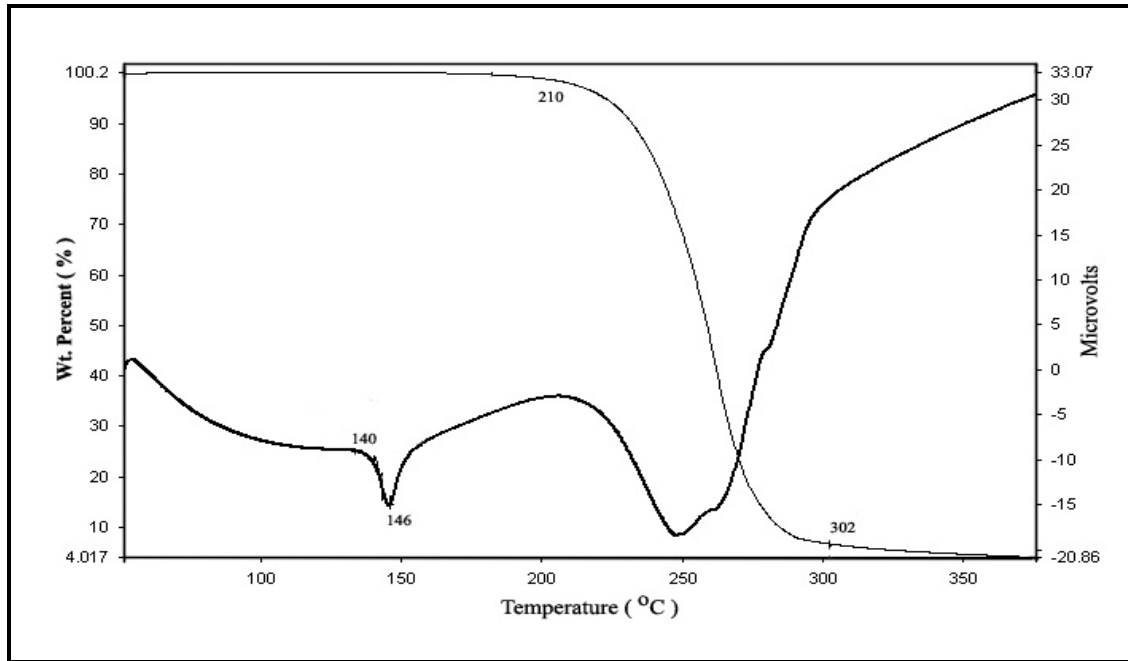


Fig. 6. TG and DTA thermograms of MAN crystal

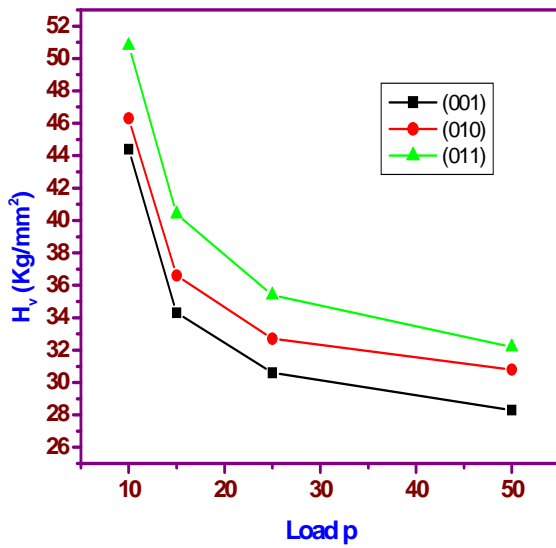


Fig. 7a. Variation of Vickers hardness number with load for MAN crystal along (0 0 1), (0 1 0) and (0 1 1) planes

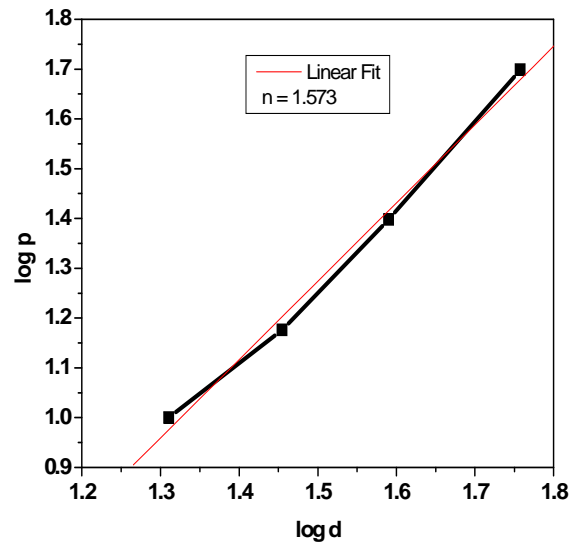


Fig. 7b. Plot of  $\log d$  Vs  $\log p$  for MAN single crystal along (0 0 1) plane

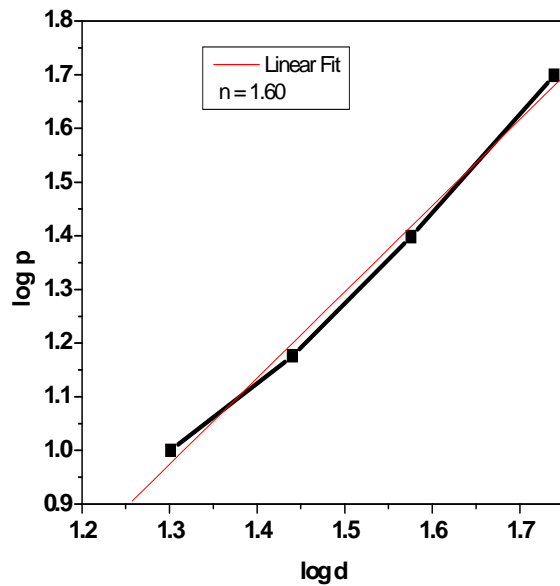


Fig. 7c. Plot of log d Vs log p for MAN single crystal along (0 1 0) plane

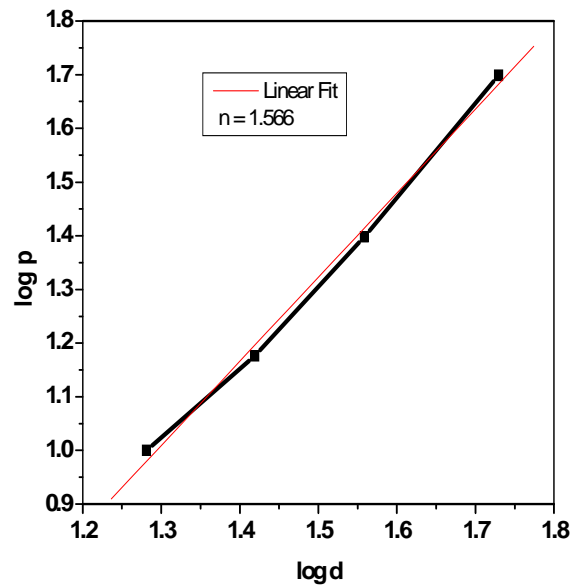


Fig. 7d. Plot of log d Vs log p for MAN single crystal along (0 1 1) plane

### 3.6 Microhardness test

The Vickers microhardness measurement was carried out on the grown crystal to estimate its hardness. Microhardness study was done Vickers microhardness tester fitted with a diamond pyramidal indenter. The static indentation tests were made on (0 0 1), (0 1 0) and (0 1 1) planes of the crystal at room temperature. The applied load was varied from 10 to 50 gm for a constant indentation period of 10 s. The variation of  $H_v$  with applied load is shown in Fig. 7a. The graph indicates that the microhardness number decreases with increasing load. The value of the work hardening coefficient 'n' was estimated from the plot of log P versus log d (Figs. 7b-7d) by the least square fit method. The value of 'n' is found to be 1.573, 1.60 and 1.566 for (0 0 1), (0 1 0) and (0 1 1) planes respectively. For specimens showing increase in  $H_v$  with increasing P, the Meyer index  $n > 2$ , which confirms the normal ISE behaviour [17]. Since the value of n for MAN is greater than 2, the hardness of the material is found to increase with applied load further confirming the prediction of [18].

### 3.7 Dielectric study

Figs. 8a and 8b show the variations of the dielectric constant and dielectric loss of MAN crystal as a function of frequency at different temperatures (308, 328, 348, 368 and 388 K). The dielectric constant of the sample is found to be 350.94 at 50 Hz and it decreases to 115.54 at 5 MHz. The very high value of  $\epsilon_r$  at lower frequencies may be due to the space charge polarization. It is evident from Fig. 8b that the crystal has a very low dielectric loss in the high frequency region, which indicates the lesser number of defects in the crystal. The variation in the value of  $\epsilon_r$  is marginal in the frequency range 1 kHz-5 MHz. It is further observed that both the dielectric constant (Fig. 8c) and dielectric loss increase with temperature.



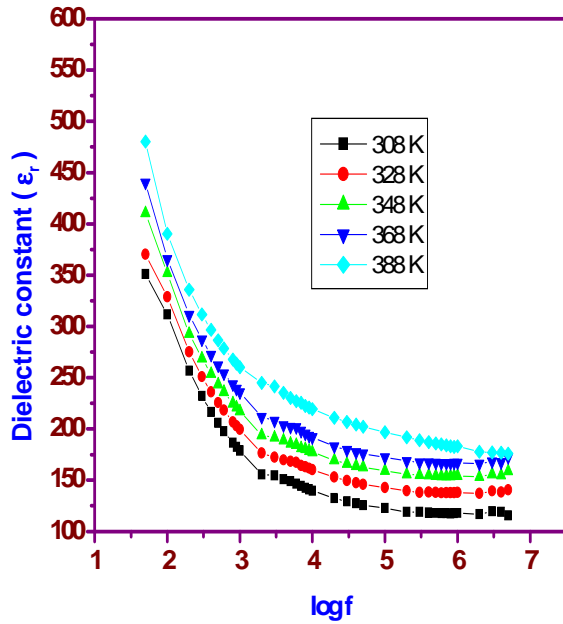


Fig. 8a. Variation of dielectric constant with log frequency at different temperatures for MAN crystal

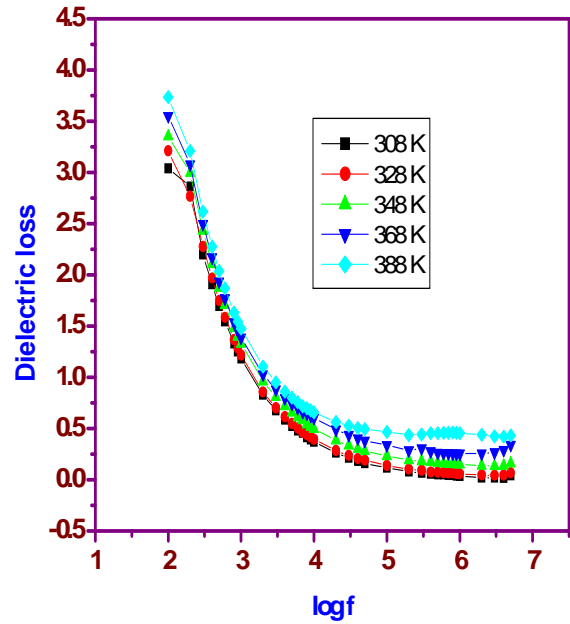


Fig. 8b. Variation of dielectric loss with log frequency at different temperatures for MAN crystal

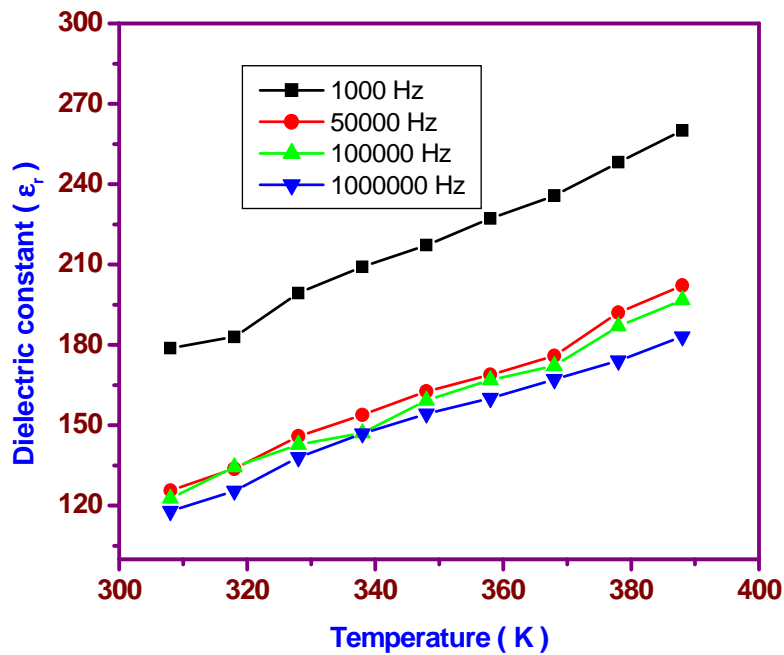


Fig. 8c. Temperature dependence of dielectric constant for MAN single crystal

### 3.8 Photoconductivity study

Photoconductivity study of the MAN single crystal was carried out by using Keithly 485 picoammeter. By not allowing any radiation to fall on the sample and by varying the applied field from 100 to 4000 V/cm, the corresponding dark current values shown by the picoammeter were recorded. To measure the photo current, the sample was illuminated with a halogen lamp (100 W) containing iodine vapour by focussing a spot of light on the sample with the help of a



convex lens. The applied field was increased from 100 to 4000 V/cm and the corresponding photo current was recorded. The photo current and dark current are plotted as a function of the applied field (Fig. 9). It is observed from the plot that the dark current is always higher than the photo current, thus confirming the negative photoconductivity. This phenomenon can be attributed to generation of mobile charge carriers caused by the absorption of photons.

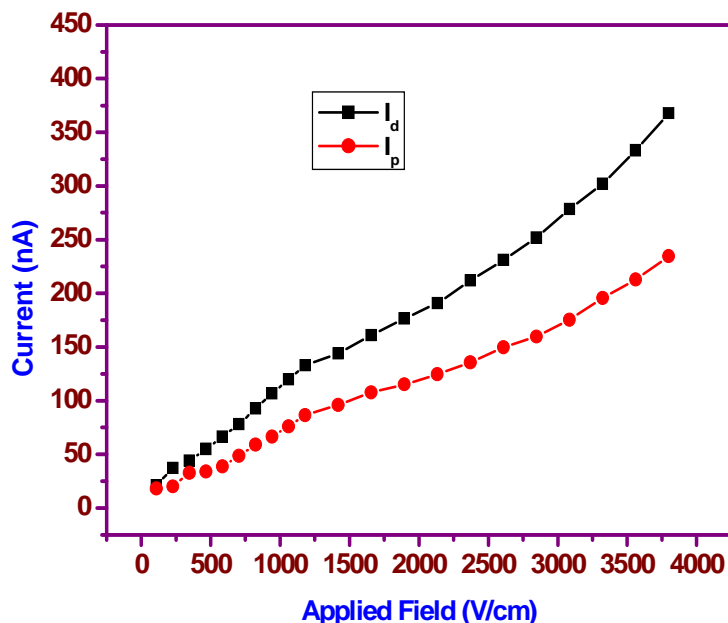


Fig. 9. Field dependent photoconductivity of MAN single crystal

## CONCLUSION

Single crystals of MAN were grown in bulk size by low temperature solution growth technique under optimized growth conditions. It was found estimated from the X-ray diffraction studies that the crystals are orthorhombic and belong to  $P2_12_12_1$  space group. The UV-Vis-NIR spectrum reveals the wider transmission window of the sample. The thermal analyses confirm the single stage weight loss of MAN crystal. It is observed from the microhardness studies that the  $H_v$  value decreases with increasing load for MAN sample and it is found to be a hard material. The hardness anisotropic nature of the crystal is confirmed by the hardness studies. The low dielectric loss with high efficiency implied that the sample possesses good optical quality with lesser defects. The photoconductivity study reveals the negative photoconducting nature of the sample. A comparatively good optical property combined with favourable NLO properties make MAN crystal as a candidate material for future applications.

## Acknowledgement

The authors acknowledge Department of Science and Technology (DST), India for funding this research project. The author C.K.M. thanks the Council of Scientific and Industrial Research (CSIR), New Delhi for the grant of a Major Research Project.

## REFERENCES

- [1] Jun Shen, Jimin Zheng, Yunxia Che, Bin Xi, *J. Cryst. Growth*, **2003**, 257, 136.
- [2] D. Xu, M. H. Jiang, Z. S. Shao, X. T. Tao, *Synth. Cryst.*, **1987**, 16, 1.
- [3] G. C. Xing, M. H. Jiang, Z. S. Shao, *Chin. Phys. Lasers*, **1987**, 14, 1.

- [4] N. Zhang, M. H. Jiang, D. R. Yuan, D. Xu, X. T. Tao, Z. S. Shao, *J. Cryst. Growth*, **1990**, 102, 581.
- [5] P. R. Newman, L. F. Warren, P. Cunningham, T. Y. Chung, D. E. Copper, G. L. Burdge, P. Polak Dingels, C. K. Lowe Ma, *Mater. Res. Soc. Symp. Pro.* **1990**, 173, 557.
- [6] Tanusri Pal, Tanusree Kar, Xin- Qiang Wang, Guang- Ying Zhou, Dong Wang, Xiu-Feng Cheng, Zhao- He yang, *J. Crystal Growth*, **2002**, 235, 523.
- [7] Reena Ittyachan, P. Sagayaraj, *J. Crystal Growth*, **2003**, 249, 557.
- [8] D. Rajan Babu, D. Jayaraman, R. Mohan Kumar, R. Jayavel, *J. Crystal Growth*, **2002**, 245, 121.
- [9] M. Vimalan, A. Ramanand, P. Sagayaraj, *Crystal Research and Technology*, **2007**, 42, 1091.
- [10] S. Natarajan, S. A. Martin Britto, E. Ramachandran, *Crystal Growth & Design*, **2006**, 6, 137.
- [11] van Nemeč, Ivana Cisarova, Zdenek Micka, *J. Molecular Structure*, **1999**, 476, 243.
- [12] A. Pricilla Jeyakumari, S. Dhanuskodi, S. Manivannan, *Spectrochim. Acta Part A*, **2006**, 63, 91.
- [13] S. Aruna, G. Bhagavannarayana, P. Sagayaraj, *J. Crystal Growth*, **2007**, 04, 184.
- [14] Tanusri Pal, Tanusree Kar, *J. Crystal Growth*, **2002**, 234, 267.
- [15] M. Gulam Mohamed, K. Rajarajan, G. Mani, M. Vimalan, K. Prabha, J. Madhavan, P. Sagayaraj, *J. Crystal Growth*, **2007**, 300, 409.
- [16] K. Ambujam, K. Rajarajan, S. Selvakumar, I. Vetha Potheher, Ginson P. Joseph, P. Sagayaraj, *J. Crystal Growth*, **2006**, 286, 440.
- [17] K. Sangwal, *Materials Chemistry and Physics*, **2000**, 63, 145.
- [18] E.M. Onitsch, *Mikroskopie*, **1956**, 95, 12.